10th International IFAC Symposium on
Computer Applications in Biotechnology
Preprints Vol.1, June 4-6, 2007, Cancún, Mexico

ADVANCED DYNAMICAL RISK ANALYSIS FOR MONITORING ANAEROBIC DIGESTION PROCESS

Jonathan Hess [*,1] **Olivier Bernard** [*]

[*] *French Research Institute of Computer Science and Automatic Control. COMORE Research Team. Sophia Antipolis 06902, France. e-mail : olivier.bernard@inria.fr, jonathan.hess@inria.fr*

Abstract: In this paper we study an unstable biological process used for waste water treatment. This ecosystem can have two locally stable equilibria and an unstable one. We first introduce the model and recall its main properties. We then study the phase plane and split it into fifteen zones according to the sign of the derivatives of the state vector. Then we propose a methodology to monitor in real-time the trajectory of the system across these zones and determine its position in the plane. We finally define a dynamical risk index based on the transitions from one zone to another and classify the zones according to their dangerousness. It is worth noting that the proposed approach do not rely on the value of the parameters and is thus very robust.

Keywords: Anaerobic digestion, non-linear system diagnosis, Haldane model, risk index.

1. INTRODUCTION AND MOTIVATION

Anaerobic digestion is a more and more popular bioprocess (Angelidaki et al. [2003]) that at the same time treats wastewater and produces energy through methane (CH_4) and hydrogen. This complex ecosystem involves more than 140 bacterial species (Delbès et al. [2001]) that progressively degrade the organic matter into carbon dioxide (CO_2) and methane (CH_4). However this process is known to be very delicate to manage since it is unstable (Fripiat et al. [1984]): an accumulation of intermediate compounds can lead to the acidification of the digester.

The objective of this paper is to analyze and characterize the dynamics of such an unstable system, in order to better assess the risk of going toward process acidification. In a previous paper (Hess and Bernard [Submitted]), a static criterion based on the size of the attraction basin of the useful working point was proposed. This criterion was however independent of the real state of the process. Here we propose to identify, on the basis of the qualitative analysis of some monitored signals (like e.g. methane flow rate) the region of the state space where the system lies. The robustness of these regions to an increase of the loading is then studied and leads to a dynamical risk criterion.
The proposed methodology relies on a mathematical analysis, but as in Hess et al. [2006] it is devoted to be applied to on-line monitoring of industrial processes.

The paper is composed as follows: in the second section the dynamical model considered for anaerobic digestion process is detailed. The third part puts the emphasis on the analysis of the model

[1] J.Hess is funded both by ADEME and by the Provence-Alpes-Cotes-d'Azur Region.

dynamics. Transitions graphs that describe the possible commutations between regions are produced in a fourth part. Finally, a risk criterion to assess the stability of the process is proposed.

2. MODEL DEFINITION AND ANALYSIS

2.1 Model presentation

We consider a generic macroscopic model of a one-stage anaerobic process where an organic substrate s is degraded by a bacterial consortium x into methane:

$$k\,s \overset{\mu(.)\,x}{\longrightarrow} x + k_G\,CH_4$$

The dynamical mass-balance model in a continuous fixed-bed reactor is straightforwardly derived:

$$\begin{cases} \dot{s} &= D\,(s_{in} - s) - k\,\mu(.)\,x \\ \dot{x} &= \mu(.)\,x - \alpha\,D\,x \\ q_m &= k_G\,\mu(.)\,x \end{cases} \tag{1}$$

where D is the dilution rate, s_{in} the influent substrate concentration, α the fraction of free biomass in the liquid medium (the rest of the biomass is attached to a support), q_m the methane molar flow rate, and, k and k_G are pseudo-stoichiometric coefficients representing respectively the substrate degradation and the methane production yields. $\mu(.)$ is the bacterial growth rate.

We will consider an Haldane-like growth rate:

$$\mu(s) = \mu_m \frac{s}{s + k_s + \frac{s^2}{k_i}} \tag{2}$$

k_i being the inhibition constant, k_s the half-saturation one and μ_m the specific growth rate.

2.2 Positivity and boundedness

This type of model has been widely described for $\alpha = 1$(Andrews [1968]) and we only recall the main properties of system (1).

For the rest of our study we assume that D and s_{in} are piecewise constant. Hence D, s_{in} and the initial values of the variables are positive.

Property 1. System (1) with initial conditions $\xi_0 = (s_0, x_0)$ in $\mathbb{R}^2_+$ remains positive and bounded at all time.

Proof: We only give the sketch of the proof. Since $\mu(0) = 0$, it is trivial to show the positivity of the system. To show the boundedness we have to consider the variable $z = s + k\,x$ and study its dynamics as exposed in Hess et al. [2006].

In the next section we present a short analysis of the model equilibria and its stability.

2.3 Equilibrium and stability

Considering the non-monotonic growth rate of equation (2), System (1) is close to a generic Haldane model, but slightly modified by the term α. Equilibria $\xi^* = (s^*, x^*)$ other than the acidification $\xi^\dagger = (s_{in}, 0)$ are solution of the following system:

$$\begin{cases} \mu(s^*) &= \alpha D \\ x^* &= \frac{s_{in} - s^*}{\alpha k} \\ \mu(s) &= \mu_m \frac{s}{s + k_s + \frac{s^2}{k_i}} \end{cases} \tag{3}$$

Several cases are possible (Hess et al. [2006]), depending on the parameters and operating conditions; one case of special interest is when there are two steady-states in the interior domain [2] , one of which along with the acidification one is locally stable (*c.f.* Figure 1).

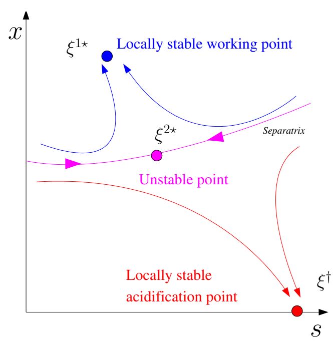

Fig. 1. Possible orbits in the phase plane.

Definition For $\xi^{1\star}$, the interior critical point of system (1), we define its **basin of attraction** $\mathcal{B}^{1\star}$as the set of initial conditions in $\mathbb{R}^2_+$ converging asymptotically towards it:

$$\mathcal{B}^{1\star} = \left\{ \xi_0 \in \mathbb{R}^2_+ \mid \lim_{t\to+\infty} \xi(\xi_0, t) = \xi^{1\star} \right\},$$

We define in the same way for $\xi^\dagger$:

$$\mathcal{B}^{\dagger} = \left\{ \xi_0 \in \mathbb{R}^2_+ \mid \lim_{t\to+\infty} \xi(\xi_0, t) = \xi^{\dagger} \right\}$$

The separatrix is defined as the variety dividing the plane into the two attraction basins (it is indeed the stable manifold associated to the unstable steady state ξ^{2*}).

Ideally the plant manager should choose operating conditions that maximise $\mathcal{B}^{1\star}$, the attraction basin of the normal operating mode $\xi^{1\star}$, in order to limit the risk of destabilisation. Yet in practice the operator has to simultaneously process a maximal loading and prevent a plant failure.

Being able to determine on what side of the separatrix the system evolves is capital to ensure

[2] here we do not consider the simpler case where there is only one interior equilibrium which is globally stable.

the stability of the process: for example if a change in the operating conditions triggers the system in the acidification attraction basin, the plant manager has to take appropriate measures to prevent the acidification of the plant.

In the sequel we seek criteria to characterize the two attraction basins, describe the dynamical behaviour of the system and evaluate on which side of the separatrix the system evolves.

3. STUDY OF THE PHASE PLANE

3.1 Partitioning of the phase plane

In the same spirit than in Bernard and Gouzé [2002], we analyse the dynamical qualitative behaviour of the system by splitting the phase plane into regions where the variables have a fixed trend. We thus split the phase plane (s, x) using the nullclines, the separatrix and the lines $s = s^m$ and $x = x^m$ (see [3] [4]) as shown on Fig. 2.

These varieties define 17 regions [5] where the sign of $(\dot{x}, \dot{s}, \dot{\mu})$ is constant. We consider in addition the nullcline $\dot{q}_m = 0$. We gather some zones with similar characteristics and we consider in the sequel only 15 zones (see Fig. 2). The qualitative characteristics $(\dot{x}, \dot{s}, \dot{\mu}, \dot{q}_m)$ of this phase plane are summarized in Table 1. It is worth noting that the q_m-nullcline almost coincides with the s-isocline in zone 1.

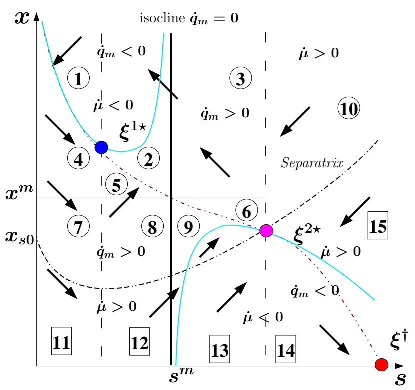

Fig. 2. Phase plane with the separatrix and the nullclines for s, x and q_m.

[3] s^m is the value that maximises the growth rate $\mu(s)$,
[4] x^m is the intersection of the s-nullcline with the line $s = s^m$
[5] a numerical study for a wide range of operating conditions ($D \in [.1; 1.05]\, d^{-1}$ and $s_{in} \in [3; 200]\, mmol.L^{-1}$) of the relative position of x^m with respect to the intersection of the separatrix and the axis $x = 0$ (called here x_{s0}) shows that the inequality $x^m > x_{s0}$ always holds.

Table 1. Qualitative signature of the subdivisions of the phase plane.

sign \ zone	1	2	3	4	5	6	7	8
$\dot{x}$	-	+	+	-	+	+	-	+
$\dot{s}$	-	-	-	+	+	-	+	+
$\dot{\mu}$	-	-	+	+	+	+	+	+
$\dot{q}_m$	-	?	+	+	+	+	+	+

sign \ zone	9	10	11	12	13	14	15
$\dot{x}$	+	-	-	+	+	-	-
$\dot{s}$	+	-	+	+	+	+	-
$\dot{\mu}$	-	+	+	+	-	-	+
$\dot{q}_m$	?	+	+	+	?	-	?

With this partitioning we see that the sign of the vector $(\dot{x}, \dot{s}, \dot{\mu}, \dot{q}_m)$ at an instant is not sufficient to identify in which zone the system lies: for example zone 5, 8 and 12 have the same qualitative signature (+,+,+,+). Indeed only four groups of zones (1, 2, 3+6 and 14) have a unique signature. For the other zones, similar qualitative characteristics may correspond to zones on both side of the separatrix as shown in Table 2.

Table 2. Indistinguishable zones on the basis of the sign of vector $(\dot{x}, \dot{s}, \dot{\mu}, \dot{q}_m)$.

zones with similar characteristics				
in $\mathcal{B}^{1\star}$	4 and 7	5 and 8	9	10
in $\mathcal{B}^{\dagger}$	11	12	13	15

As the instantaneous trends do not provide a precise positioning of the trajectory at time t, we will now study the successive transitions between these regions and show that they can clear up the ambiguities.

3.2 Dynamical evolution of the system

We consider the complete phase plane of Figure 2 and we determine, according to the vectors field, the possible transitions of the trajectories [6] from one zone to another. This leads to transitions graphs (Bernard and Gouzé [2002]), as represented on Figures 3. Since the trajectories are bounded, it is worth remarking that they cannot stay trapped in a zone, unless they reach a steady state. This is possible only from zone 2, 4 or 14. Indeed in $\mathcal{B}^{1\star}$, zone 2 is the only region beyond the steady-state in s where the substrate decreases, and zones 4 (in $\mathcal{B}^{1\star}$) and 14 (in $\mathcal{B}^{\dagger}$) the only regions below the equilibrium in s where s is increasing.

It is worth noting that a minimum of the gas flow rate (m_q) can be observed only in $\mathcal{B}^{1\star}$.

The transitions graph for $\mathcal{B}^{\dagger}$ clearly shows that after a transient time the system enters zone 14 which is a dead-end. Once system (1) enters this

[6] we neglect the zero dimensional set of trajectories that cross 2 zones at the same time.

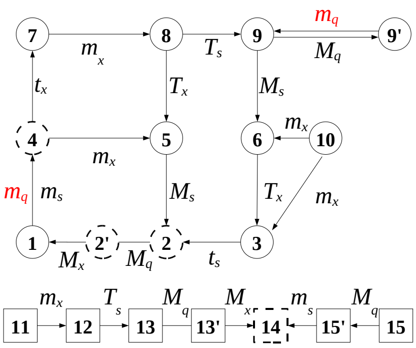

Fig. 3. Possible dynamical trajectories and transitions of the system in $\mathcal{B}^{1\star}$ (upper figure), $\mathcal{B}^{\dagger}$ (lower figure). M symbolizes a transition through a maximum, m a transition through a minimum, and T and t respectively an increasing and decreasing transition through the lines $x = x^m$ or $s = s^m$.

part of the plane it can only converges towards the acidification equilibrium. On the contrary there exist possible cycles and no clear terminal zone for $\mathcal{B}^{1\star}$: the convergence towards the normal equilibrium $\xi^{1\star}$ appears less straightforward and thus even with favorable initial conditions, the system can pass through zones close to the separatrix before converging.

The convergence towards $\xi^{1\star}$ is only possible in zone 2 and 4 and as such these two zones are relatively safe. Nevertheless zone 1 is characterized by a high biomass and a decreasing substrate (see Table 1) and as such it can be considered as one of the safest part of the plane. We then propose a risk index associated to the minimal number of zones the system has to cross (*i.e* the number of transitions) before reaching the *converging regions*. In the same way for $\mathcal{B}^{\dagger}$, we classify the risk by the number of transitions before the system reaches zone 14. Table 3 presents this ranking.

Table 3. Risk ranking of the phase plan (I.R.: inhibition region, C.R.: convergence region, E.Z.: exit zone).

Risk	Ranking	Nb of transitions	Zone	Comments
	1	0	2	C.R.
	2	1	1	
	3	1	5	
	4	0	4	C.R., E.Z.
	5	2	3	I.R.
	6	2	8	
	7	2	6	I.R.
	8	3	7	
	9	3	9	I.R.
	10	4	10	I.R.
	11	3	11	
	12	2	12	
	13	1	13, 15	I.R.
	14	0	14	I.R., C.R.

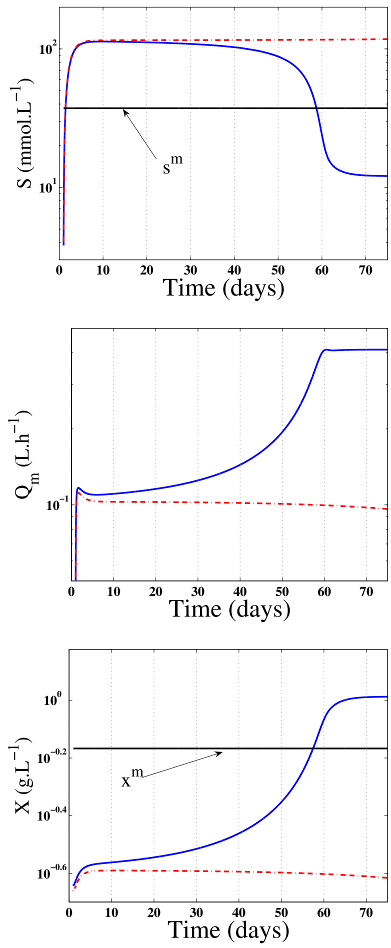

Fig. 4. Simulation of the fictive trajectories with close initial conditions (s_0 in mmol.L^{-1}, x_0 in g.L^{-1}) on both side of the separatrix; (3.81,0.23)[-], (3.81,0.22)[-.] .

3.3 Dynamical follow-up of the system

Here we demonstrate that the qualitative dynamical follow-up of a trajectory allows to identify the system position in the phase plane. In order to illustrate this approach we consider two possible fictive trajectories initialised on both side of the separatrix; the first sequence characterizes a trajectory in $\mathcal{B}^{1\star}$ initialized in region 7 and the second one a trajectory in $\mathcal{B}^{\dagger}$ initialized in 11. The transitions sequences according to the transitions graphs of Fig. 3 are the following:

in $\mathcal{B}^{1\star}$	in $\mathcal{B}^{\dagger}$
$m_x \to T_s \to M_q \to m_q \to M_s \to T_x \to t_s$	$m_x \to T_s \to M_q \to M_x$

For these two examples we see that the first three transitions ($m_x \to T_s \to M_q$) are the same for both trajectories, while the fourth transition discriminates the two trajectories.

As a consequence, if we monitor the trends, *i.e.* the sign of $(\dot{x}, \dot{s}, \dot{\mu}, \dot{q}_m)$ on a sufficiently long period we can identify the region of the space where the system is, and identify the associated risk, but we

can also assess the trajectory history. For example we see on Fig. 4 that close initial conditions can lead to opposite final state. More interesting is that the successive extrema and transitions are easily seen on Fig 4 and the fourth transitions (m_q in $\mathcal{B}^{1\star}$ or M_x in $\mathcal{B}^{\dagger}$) which are decisive to discriminate the two trajectories can be detected before the system reaches its steady state.
It is worth noting that this property is generic and does not depend on the parameters values. This approach can then be applied even without knowing the model parameters.

3.4 Qualitative monitoring with partial available information

So far the analysis was done assuming that all the variables were measured (even qualitatively) which is not realistic in practice. In practice only the substrate s and the gas flow rate q_m may be easily measured. If only the trends for s and q_m are detected, we can derive sub-graphs from the transitions graphs of Fig. 3 (see Fig. 5).

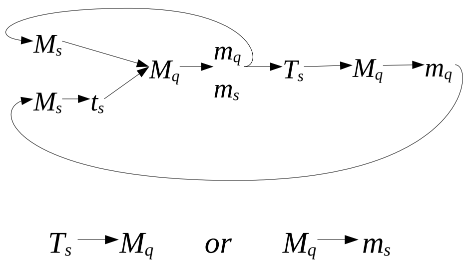

Fig. 5. Transitions sequences in $\mathcal{B}^{1\star}$ (upper figure) and $\mathcal{B}^{\dagger}$ (lower figure) with partial knowledge of the state.

This shows that any **sequence of three transitions** is decisive to qualitatively identify the state of the system. Indeed a sequence of two transitions is not sufficient as the sequence $T_S \rightarrow M_q$ is possible in the two basins (zone 8 to zone 9 in $\mathcal{B}^{1\star}$ or zone zone to zone 13 in $\mathcal{B}^{\dagger}$). It is a problem because in $\mathcal{B}^{\dagger}$ these transitions eventually lead to the acidification steady-state. However it is worth noting that this sequence corresponds to a low biomass and a relatively high substrate. As such it is a situation that the operator should detect easily.

3.5 Evolution of the phase plane after a change in the operating conditions

The previous analysis holds for piecewise constant operating conditions. A change in D or s_{in} will affect the phase plane: the equilibria are likely to move, and the nullclines and the separatrix will move either. The zones will change and we have to consider the new phase plane to asses the stability of the process.

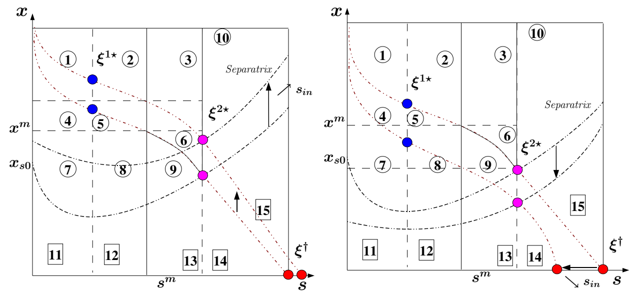

Fig. 6. Evolution of the phase plane with an increase in s_{in} (left figure), a decrease in s_{in} (right figure).

Here we consider that D is constant [7] and we study how the phase plane evolves after a change in s_{in}.

First let us remark that $x^{\star}$ is the only equilibrium changing with s_{in} (*c.f.* system (3)). Thus the vertical nullclines on Figure 2 do not evolve, but the separatrix, the equilibria and the s-nullcline will "move" vertically. We give on Fig. 6 a sketch of how the phase plane could change respectively after an increase (left figure) or a decrease (right figure) of the influent substrate concentration.

The possible switch from one zone to another are summarized on Fig. 7: a point in a zone either stay in the same zone or shifts to an adjacent zone. It is illustrated on Fig. 6 (left graph) where after the increase of s_{in} most of the former zone 7 has slided into the attraction basin of the acidification equilibrium.

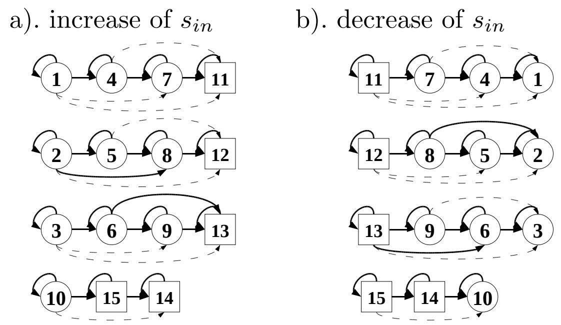

Fig. 7. Possible dynamical evolution of the zones with an increment in s_{in}.

If we consider that only small changes in s_{in} can occur we can restrict this study to adjacent zones transitions (thick plain arrows on Fig. 7). We see that a step-change in s_{in} might not endanger the process stability depending on the position of the system at the time of the perturbation.

[7] or at least that its variations are slow in comparison to the changes in s_{in}.

3.6 Destabilisation ranking

According to the possibility of slipping out of $\mathcal{B}^{1\star}$ into $\mathcal{B}^{\dagger}$ after an increasing step-change in s_{in} we grade the dangerousness of each zone in $\mathcal{B}^{1\star}$: the more changes of s_{in} are necessary, the more robust is the zone to perturbations in the influent substrate. At the opposite for $\mathcal{B}^{\dagger}$ we classify the zones considering the minimal number of decreasing step-changes that are necessary for a zone to slip in $\mathcal{B}^{1\star}$.

Table 4. Risk of destabilisation after a step-increase of s_{in} (I.R.: inhibition region, C.R.: convergence region).

Risk	Ranking	Nb of step changes	Zone	Comments
	1	3	1,2	
	2	2	4,5	
	3	3	3	I.R.
	4	1	6	I.R.
	5	1	7,8	
	6	1	9, 10	I.R.
	7	1	11, 12	
	8	1	13, 15	I.R.
	9	1	14	I.R., C.R.

4. GLOBAL RISK INDEX

We propose to combine the two risk rankings presented previously (Tab. 3 and 4) in order to build a global grading of the dangerousness of a zone taking into account:

- the "distance" (in terms of numbers of transitions) to the steady state $\xi^{1\star}$,
- and the qualitative stability of the zones in $\mathcal{B}^{1\star}$.

To do so we sum for each zone its rank associated to each risk, and order the zones with this index: $2 \ll 1 \ll 5 \ll 4 \ll 3 \ll 8 \ll 6 \ll 7 \ll 9 \ll 10 \ll 11 \ll 12 \ll 13,\ 15 \ll 14$

This classification can be used to inform the operator of the process of the risk on a gradual scale.

5. CONCLUSION

In this paper we have studied the dynamical behaviour of a simple model of anaerobic digestion. We have shown how qualitative events such as extrema or crossing of some values can be used to identify in which part of the space the trajectory lies even on the basis of a partial qualitative knowledge. Moreover with the monitoring of the trends of some variables, for example the sign of $(\dot{s}, \dot{q}_m)$, we can assess an associated dynamical risk. Thereby this methodology completes the static criterion presented in Hess et al. [2006] that demonstrated its efficiency on real data.

The next step would then consists in validating our dynamical risk analysis on a real process.

A possible application of this method could be the progressive increase of the loading rate of a digester in a start-up phase. Indeed, it provides a criterion to check that the plant properly reacts to the increasing load. The approach could for example help in improving the start-up protocol presented in Steyer et al. [1999] based on qualitative disturbances monitoring.

It is worth noting that the presented properties are rather generic and do hardly depend on the parameter values. This approach can then be applied even without knowing the model parameters and is thus very robust.

Acknowledgement: J.Hess is funded both by ADEME and by the Provence-Alpes-Cotes-d'Azur Region.

REFERENCES

J. F. Andrews. A Mathematical Model for the Continous Culture of Microorganisms Utilizing Inhibitory Substrates. *Biotechnology and Bioengineering*, 10:707–723, 1968.

I. Angelidaki, L. Ellegaard, and B. K. Ahring. *Biomethanation II*, chapter Applications of the anaerobic digestion process, pages 1–33. Springler, 2003.

O. Bernard and J.-L. Gouzé. Global qualitative behavior of a class of nonlinear biological systems: application to the qualitative validation of phytoplankton growth models. *Artif. Intel.*, 136:29–59, 2002.

C. Delbès, R. Moletta, and J.-J. Godon. Bacterial and archaeal 16s rdna and 16s rrna dynamics during an acetate crisis in an anaerobic digestor ecosystem. *FEMS Microbiology Ecology*, 35:19–26, 2001.

J.L. Fripiat, T. Bol, H. Naveau R. Binot, and E.J. Nyns. A strategy for the evaluation of methane production from different types of substrate biomass. In R. Buvet, M.F. Fox, and D.J. Picker, editors, *Biomethane, Production and uses*, pages 95–105. Roger Bowskill ltd, Exeter, UK, 1984.

J. Hess and O. Bernard. Design and study of a risk management criterion for an unstable anaerobic wastewater treatment process. *Journal of Process Control*, Submitted.

J. Hess, O. Bernard, and M. Djuric. A risk management criterion for an unstable wastewater treatment process. Gramado, Brazil, April 2^{th}–6^{th} 2006. ADCHEM, Elsevier.

J.-Ph. Steyer, P. Buffière, D. Rolland, and R. Moletta. Advanced Control of Anaerobic Digestion Processes through Disturbances Monitoring. *Water Research*, 33(9):2059–2068, 1999.